

Critical and tricritical singularities of the three-dimensional random-bond Potts model for large q

M. T. Mercaldo,¹ J-Ch. Anglès d'Auriac,² and F. Iglói^{3,4}

¹*Dipartimento di Fisica “E.R. Caianiello” and Istituto Nazionale per la Fisica della Materia, Università degli Studi di Salerno, Baronissi, Salerno I-84081, Italy*

²*Centre de Recherches sur les Très Basses Températures, B. P. 166, F-38042 Grenoble, France*

³*Research Institute for Solid State Physics and Optics, H-1525 Budapest, P.O.Box 49, Hungary*

⁴*Institute of Theoretical Physics, Szeged University, H-6720 Szeged, Hungary*

(Dated: May 9, 2018)

We study the effect of varying strength, δ , of bond randomness on the phase transition of the three-dimensional Potts model for large q . The cooperative behavior of the system is determined by large correlated domains in which the spins points into the same direction. These domains have a finite extent in the disordered phase. In the ordered phase there is a percolating cluster of correlated spins. For a sufficiently large disorder $\delta > \delta_t$ this percolating cluster coexists with a percolating cluster of non-correlated spins. Such a co-existence is only possible in more than two dimensions. We argue and check numerically that δ_t is the tricritical disorder, which separates the first- and second-order transition regimes. The tricritical exponents are estimated as $\beta_t/\nu_t = 0.10(2)$ and $\nu_t = 0.67(4)$. We claim these exponents are q independent, for sufficiently large q . In the second-order transition regime the critical exponents $\beta_t/\nu_t = 0.60(2)$ and $\nu_t = 0.73(1)$ are independent of the strength of disorder.

I. INTRODUCTION

The effect of bond randomness on the critical behavior of ferromagnetic models is well understood if the non-random system has a second-order phase transition¹. Much less is known, however, if this transition is discontinuous². In two dimensions (2d) rigorous results asserts that for any type of continuous disorder the transition softens into a second order one³. Recent numerical studies of the 2d q -state random bond Potts model⁴ (RBPM) have shown that the magnetization exponent of this model is q -dependent^{5,6} and saturates^{7,8} for large- q at a possibly exactly known value^{9,10}. On the other hand the energy exponent, ν , is found to show only a very weak variation with q .

In real 3d systems the effect of bond randomness is more complex and here we are lacking rigorous results. It is demonstrated experimentally that the isotropic to nematic transition of nCB liquid crystal turns to second order for sufficiently strong disorder¹¹. The same type of softening effect is found in Monte Carlo simulations for the $q = 3$ and $q = 4$ Potts models, both for site^{12,13} and bond dilution¹⁴. With very large computational effort it was possible to locate the second order transition point and to estimate the critical exponents, which are found q dependent both for the magnetization and for the energy density.

The first-order transition regime (for weak disorder) and the second-order transition regime (for strong disorder) are separated by a tricritical point the properties of which are conjectured to be related to the critical point of the random field Ising model (RFIM). As shown by Cardy and Jacobsen⁶ in the limit of $d \rightarrow 2$ and $q \rightarrow \infty$ the interface Hamiltonian of the two problems have the same type of solid-on-solid (SOS) description, from which follows that the energy exponents of the tricritical RBPM

are equivalent to the magnetization exponents of the critical RFIM. Furthermore, analyzing the renormalization group (RG) flow it was conjectured that the above mapping stays valid for $d > 2$, in particular at $d = 3$. Thus the tricritical exponents should be q independent, at least for large q , leading to the same exponents for any disorder induced tricritical points.

These conjectures, which could be of experimental relevance, have not yet been verified numerically. The inaccuracies in the simulations have mainly two sources: i) it is difficult to precisely locate the tricritical point due to strong cross-over effects and ii) for not too large q the tricritical disorder is quite small which results in large breaking-up lengths in the system¹⁰, thus one has to treat quite large lattices.

In the present paper we consider the 3d ferromagnetic Potts model¹⁵ for large value of q , which has a strongly first-order transition for non-random couplings and study the effect of bond randomness including also the case of bond dilution. In the large- q limit the high-temperature expansion of this problem¹⁶ is dominated by a single diagram¹⁷ which is exactly calculated by a combinatorial optimization method¹⁸. Weak disorder is studied perturbatively, whereas for stronger disorder we have performed extensive numerical calculations. In particular we have studied the properties of the tricritical point and checked its possible relation with the critical fixed point of the RFIM. We have also studied the form and universality, i.e. disorder independence, of the critical singularities. For these quantities some results have already been announced in a letter¹⁹.

The structure of the paper is the following. The RBPM and the optimization method used in the study for large q is presented in Sec.II. Perturbative treatment of the problem in the weak disorder limit is shown in Sec.III. Numerical results about the phase diagram as well as

on critical and tricritical singularities are given in Sec.IV and discussed in Sec.V.

II. MODEL AND ITS PHASE DIAGRAM

The q -state Potts model¹⁵ is defined by the Hamiltonian:

$$\mathcal{H} = - \sum_{\langle i,j \rangle} J_{ij} \delta(\sigma_i, \sigma_j) \quad (1)$$

in terms of the Potts-spin variables, $\sigma_i = 0, 1, \dots, q-1$. Here i and j are sites of a cubic lattice and the summation runs over nearest neighbors. The couplings, $J_{ij} > 0$, are ferromagnetic and identically and independently distributed random variables. In this paper we use a bimodal distribution:

$$P(J_{ij}) = p\delta(J(1+\delta) - J_{ij}) + (1-p)\delta(J(1-\delta) - J_{ij}) \quad (2)$$

with $p = 1/2$. The parameter $0 < \delta \leq 1$ plays the role of the strength of disorder and at $\delta = 0$ and $\delta = 1$ we recover the non-random and the diluted systems, respectively.

For a given set of couplings the partition function of the system is conveniently to write in the random cluster representation¹⁶ as:

$$Z = \sum_G q^{c(G)} \prod_{ij \in G} [q^{\beta J_{ij}} - 1] \quad (3)$$

where the sum runs over all subset of bonds, G and $c(G)$ stands for the number of connected components of G . In Eq.(3) we use the reduced temperature, $T \rightarrow T \ln q$ and its inverse $\beta \rightarrow \beta / \ln q$, which are of $O(1)$ even in the large- q limit¹⁰. In this limit we have $q^{\beta J_{ij}} \gg 1$ and the partition function can be written as

$$Z = \sum_{G \subseteq E} q^{\phi(G)}, \quad \phi(G) = c(G) + \beta \sum_{ij \in G} J_{ij} \quad (4)$$

which is dominated by the largest term, $\phi^* = \max_G \phi(G)$. Note that the optimal set itself generally depends on the temperature. The free-energy per site is proportional to ϕ^* and given by $-\beta f = \phi^*/N$ where N stands for the number of sites of the lattice.

The optimization problem in Eq.(4) contains a cost-function, $\phi(G)$, which is sub-modular²⁰ and there is an efficient combinatorial optimization algorithm, which at any temperature, works in strongly polynomial time¹⁸. This algorithm finds a set of bonds which minimizes the cost-function. We call such a set an optimal set. The variation of the optimal set with the temperature is illustrated²¹ in Fig.1 for $\delta = 0.875$ and $L = 24$. At low temperature the optimal graph is compact and the largest connected subgraph contains a finite fraction of the sites. In the other limit, for high temperature, most of the sites in the optimal set are isolated and the connected clusters have a finite extent, the typical size of which is used to define the correlation length, ξ .

Between the low-temperature (ordered) and the high-temperature (disordered) phases in the thermodynamic limit there is a sharp phase transition. The numerically calculated phase-diagram as a function of the temperature, T , and the disorder, δ , is shown in Fig. 2. A detailed analysis of the phase-diagram is postponed to Sec.IV. Here we just note that the transition is of first order for weak disorder, in which case ξ stays finite at the transition point, but the transition is of second order for strong enough disorder, when the correlation length is divergent at the transition point. This second possibility is illustrated in the central part of Fig.1, when at the transition point the largest connected cluster is a fractal and its fractal dimension, d_f , is related to the magnetization critical exponent, see in Sec.IV. The fractal dimension of the giant connected cluster at the transition point is shown in the inset of Fig. 2, as calculated in Sec.IV C. In the first-order regime it is $d_f = 3$, i.e. the cluster is compact, whereas in the second-order regime it is $d_f < 3$ and practically independent of the strength of disorder. At the tricritical disorder, δ_t , the giant cluster is a fractal but its fractal dimension is different from that in the critical regime, see in Sec.IV D.

III. PERTURBATIVE CALCULATION FOR WEAK DISORDER

A. Non-random model and Imry-Ma type argument for weak disorder

In the non-random model, $\delta = 0$, there are only two homogeneous optimal sets, which correspond to the $T = 0$ and $T \rightarrow \infty$ solutions, respectively, see in Ref.²¹. For $T < T_c(0)$ it is the fully connected diagram with a free-energy: $-\beta N f = 1 + N\beta J d$ and for $T > T_c(0)$ it is the empty diagram with $-\beta N f = N$. Consequently the transition point is located at: $T_c(0) = Jd/(1 - 1/N)$ and the latent heat is $\Delta e/T_c(0) = 1 - 1/N$.

In the presence of disorder, $\delta > 0$, the optimal sets are homogeneous only in a limited temperature range and new non-homogeneous optimal diagrams appear, see in Fig.1. In the disordered phase in the vicinity of $T_c(0)$ the typical linear size of the connected clusters, l , can be estimated along the lines of the Imry-Ma argument²². Adding to the optimal set a cluster with a number of sites of the order l^d will decrease the number of connected components, and therefore increase the cost-function by l^d . On the other hand, it will add a number of the order $dl^d - dl^{d-1}$ of bonds, each having a weight $(1 \pm \delta)/d$ since the temperature is close to $T_c(0)$. It results in a competition between a term behaving like $l^{d/2}$, which represents the gain due to disorder fluctuations and a term like l^{d-1} , which is the lost due to the creation of an interface. In $d = 2$ the two terms balance each other and extreme fluctuations of the disorder will create clusters of unlimited size¹⁰. As a consequence in $2d$ there is no coexistence of pure phases and the transition is of second

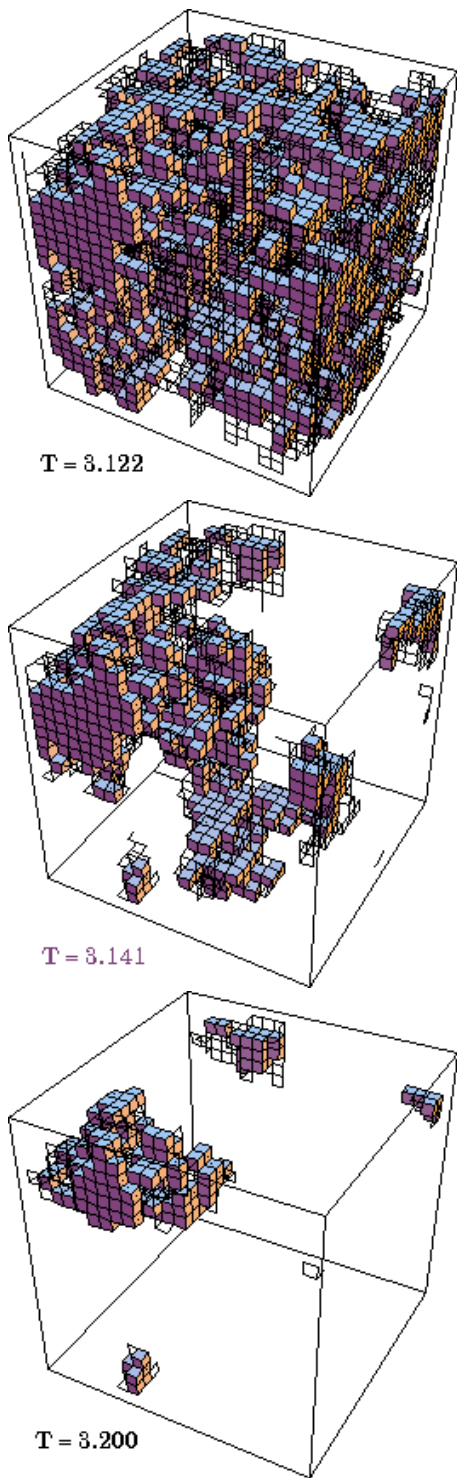


FIG. 1: Connected parts of typical optimal sets with $L = 24$ at $\delta = 0.875$. Top: $T = 3.122J < T_c$, centre: $T = 3.141J \approx T_c$ and bottom: $T = 3.200J > T_c$.

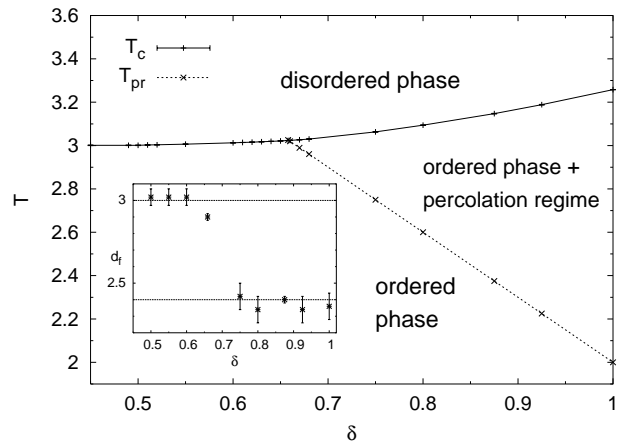


FIG. 2: Phase diagram of the random-bond Potts model for bimodal disorder. In the ordered phase in the optimal set the non-connected sites are percolating for $\delta > \delta_{pr}$ and $T_{pr}(\delta) < T < T_c(\delta)$. Numerical results indicate, that the first- and second-order transition regimes are separated by a tricritical disorder, δ_c , which corresponds to the border of the percolation regime, $\delta_c = \delta_{pr}$. Inset: fractal dimension of the giant connected cluster at the transition point as calculated in Sections IV C and IV D. The straight lines at $d_f = 3$ and $d_f = 2.40$ indicating the values at the first-order and the second-order transition regimes, respectively, are guide to the eye.

order for any small amount of disorder³.

On the contrary in $d > 2$, in particular in three dimensions for weak disorder the surface term is dominating, thus the connected clusters have a finite extent and the transition is of first-order in accordance with the phase diagram in Fig. 2. In this case connected clusters are created due to extreme fluctuations of disorder, and the statistics of these rare regions will be considered in the following subsection. A similar analysis of the ordered phase will be given afterward in Sec. III C.

B. Disordered phase

Here we make the estimate of the free-energy as simple as possible and therefore we consider rare regions of the shape of cubes of linear linear size, $l \geq 2$, in which all the $n_+ = 3(l^3 - l^2)$ internal couplings are strong, being $J(1 + \delta)$. The cost-function of the diagram in which all the bonds of the cube are present relative to the empty graph is given by:

$$\Delta f_+(l) = 3\beta(l^3 - l^2)J(1 + \delta) - (l^3 - 1). \quad (5)$$

The optimal set is then the inhomogeneous one containing the connected cluster, if $\Delta f_+(l) > 0$, which could take place if the disorder satisfies the relation, $\delta > \delta_+(l)$, with

$$\delta_+(l) = \frac{l+1}{l^2}. \quad (6)$$

In another words for a given disorder, δ , there is a limiting size, $l_+(\delta) = (1 + \sqrt{1 + 4\delta})/2\delta \approx 1/\delta$, and only large enough clusters with $l \geq l_+(\delta)$ can exist in the optimal graph. provided the temperature is in the range of $3 < T/J < T_+(l)/J = 3 + 3(\delta - \delta_+(l))/(1 + \delta_+(l))$. Thus for weak disorder only large (and very rare) clusters can be found and as the disorder is increased at discrete values of δ new, smaller and more probable connected clusters will appear. This mechanism will lead to discontinuous behavior of the free energy as a function of the disorder, which is indeed observed in numerical calculations.

The probability of having all the n_+ couplings strong in a cube is exponentially small, $P_+(l) = 2^{-n_+}$, thus the density of connected cubes of size l in the optimal set is given by $\rho_+(l) = 2^{-3(l^3+l^2)}$. The free energy of the non-homogeneous optimal set is given by the sum of contributions of the connected clusters of different size:

$$-\beta N f_+ \simeq N + N \sum_{l \geq l_+(\delta)} \Delta f_+(l) \rho_+(l). \quad (7)$$

Since $\rho_+(l)$ is a very rapidly decreasing function of l the sum in Eq.(7) is dominated by the term with $l = l_+(\delta)$.

C. Ordered phase

In the ordered phase, $T \leq T_c(0)$, we consider rare regions of extreme disorder fluctuations also of the shapes of cubes with $l \geq 1$, so that all the couplings, $n_-(l) = 3(l^3 + l^2)$, starting from the points of the cubes are weak, being $J(1 - \delta)$. The cost-function of the diagram in which all weak bonds of the cube are absent, i.e. there is a cube of isolated points embedded into the full diagram, relative to the full graph is given by:

$$\Delta f_-(l) = l^3 - 3\beta(l^3 + l^2)J(1 - \delta). \quad (8)$$

As for the disordered phase the optimal set is the inhomogeneous one containing the isolated points, if $\Delta f_-(l) > 0$, which is the case for strong enough disorder, $\delta > \delta_-(l)$, with

$$\delta_-(l) = \frac{1}{l+1}. \quad (9)$$

Now for a given disorder, δ , the limiting size is, $l_-(\delta) = 1/\delta - 1 \approx 1/\delta$, and the $l \geq l_-(\delta)$ “empty clusters” exist in the optimal graph in the range of temperature $3 > T/J > T_-(l)/J = 3 + 3(\delta - \delta_-(l))/(1 + \delta_-(l))$. Now the density of cubes of isolated points of size l in the optimal set is given by $\rho_-(l) = 2^{-3(l^3+l^2)}$ and the free energy of the non-homogeneous optimal set can be written as:

$$-\beta N f_- \simeq 1 + N\beta J d + N \sum_{l \geq l_-(\delta)} \Delta f_-(l) \rho_-(l), \quad (10)$$

which is dominated by the term with $l = l_-(\delta)$.

D. Phase transition

The phase-transition temperature, $T_c(\delta)$, is obtained by equating the free-energy in the two phases: $f_- = f_+$. Since it is comparatively easier to create an “empty cluster” in the ordered phase, than a connected cluster in the disordered phase which results in the shift of the phase boundary towards higher temperatures as the disorder is increasing, see Fig. 2. Further observation, that the phase-boundary is discontinuous at $\delta_+(l)$ and $\delta_-(l)$, for all integer l -s. For small δ , which corresponds to large l -s these jumps are very frequent and in a mathematical point of view the phase boundary is a non-analytical function of δ . However these jumps are very small and the phase-boundary can be approximated by a continuous curve which asymptotically behaves as:

$$\ln(T_c - T_c(0)) \sim -\frac{1}{\delta^3}. \quad (11)$$

We obtain similarly for the latent heat and for the jump of the magnetization at the transition point:

$$\ln(\Delta e/T_c - 1) \sim \ln(\Delta m - 1) \sim -\frac{1}{\delta^3}. \quad (12)$$

Thus the phase transition stays first order and as the disorder is switched on there is an essential singularity in the thermodynamical quantities as a function of δ^{-3} .

E. Distribution of the finite-size transition temperature

For a large finite system of linear size, L , and for a given realization of the disorder one can define a transition temperature, $T_c(L)$, at which the disordered phase and the ordered phase (having a spanning giant cluster) coexists. The distribution of $T_c(L)$ is discontinuous for a finite system but expected to be Gaussian for large L , so that characterized by its average, $T_c^{av}(L)$, and its variance, $var[T_c(L)] = [\Delta T_c(L)]^2$. The shift of the average is asymptotically given by:

$$T_c^{av}(L) - T_c(\infty) \sim L^{-1/\tilde{\nu}}, \quad (13)$$

whereas the width scales with another exponent, ν , as:

$$\Delta T_c(L) \sim L^{-1/\nu}. \quad (14)$$

These relations define the exponents ν and $\tilde{\nu}$ and hold for second order^{23,24,25,26,27} as well as for first order phase transitions^{28,29}. At a first-order transition what we study here $\tilde{\nu}$ is just the discontinuity fixed point value of the correlation length exponent^{30,31} and given by $\tilde{\nu} = \nu_d = 1/d$. This exponent describes the variation of a diverging length-scale which can be measured in a *typical sample*. The width of the distribution can be obtained from the consideration that the density of clusters, ρ_{\pm} , has a fluctuation in finite systems which has a

TABLE I: Breaking-up disorder in the ordered phase: comparison of the interpolation formula in Eq.(15) with numerical results

L	δ_{int}^b	δ_{num}^b
7	0.466	0.469
9	0.454	0.458
15	0.434	0.438
17	0.430	0.435
23	0.420	0.429
31	0.412	0.423
39	0.406	0.418

width of, $\Delta\rho_{\pm}(L)/\rho_{\pm} \sim \rho L^{-d/2}$, according to the central limit theorem. The fluctuations in $\Delta\rho_{\pm}(L)$ are then seen in the fluctuations of $T_c(L)$, too, leading to an exponent, $\nu = 2/d$. This exponent is related to another diverging length-scale, which can be deduced from the study of *average* quantities. Note that this length is not present in the pure system and by switching on disorder its prefactor, ρ_{\pm} , presents an essential singularity as a function of δ . These results are in accordance with the considerations presented in Sec.VII of Ref.[28]. Numerical analysis of $T_c(L)$ in for stronger disorder is given in Sec.IV.

F. Breaking-up lengths

For weak disorder the density of elementary excitations is very small and the average distance between two excitations is given by $L_+^b \sim \rho_+(\delta)^{-1/3}$ and $L_-^b \sim \rho_-(\delta)^{-1/3}$, in the two phases, respectively. L_+^b and L_-^b can be interpreted as breaking-up lengths, since in a finite system of linear size, $L < L_{\pm}^b$, the optimal set is homogeneous. Using results about the critical densities we obtain:

$$\begin{aligned} \log_2 L_+^b &= (1 + 2\delta - 2\delta^2 + \sqrt{1 + 4\delta})/2\delta^3, \\ \log_2 L_-^b &= (\delta^{-1} - 1)^3 + (\delta^{-1} - 1)^2, \end{aligned} \quad (15)$$

which in principle is valid only at $\delta = \delta_{\pm}(l)$, however as an interpolation formula we can use them for not too small δ -s, too.

It is easy to see that the breaking-up lengths in the ordered phase are much smaller, then in the disordered one. For example at the value of $\delta = 1/2$, which corresponds to the existence of a single hole in the ordered phase and to a $l = 2$ connected cube in the disordered phase, respectively, $L_-^b = 4$, whereas $L_+^b \approx 2^{13}$. We have checked the accuracy of the formula in Eq.(15) by comparing the predicted breaking-up disorder, δ_{\pm}^b , for a given size, L , with that calculated numerically. As seen in TableI there is a satisfactory agreement, even for not too small δ -s.

IV. NUMERICAL RESULTS

In the numerical calculation we have treated samples with random couplings having a cubic shape with periodic boundary conditions and a linear size $L = 16, 24, 32$. For $\delta = 0.875$ we went up to $L = 40$ and in some cases we made calculations for odd values of L , too. The free-energy as well as the magnetization is calculated exactly by the combinatorial optimization algorithm, called as ‘‘optimal cooperation’’¹⁸ and averaging is performed over several thousands of samples, for the largest size the number of realizations was several hundreds. For a fixed temperature the optimal cooperation algorithm works in strongly polynomial time. As we have already mentioned in the application of the method in $2d^{10}$ for a finite system the free-energy is a piece-wise linear function of the temperature. For the bimodal disorder the number of linear parts, N_p , is found to increase with the size of the system L as well as with the disorder strength δ . A rough estimation yields

$$N_p \simeq CL^{1+\delta}, \quad (16)$$

with the constant C around one half. We have managed to implement our method in such a way that we can calculate the free-energy in the whole temperature range, i.e. in all linear parts. Note that with the hypothesis (16) the exact calculation of the free energy *in the whole temperature range* is still polynomial, whatever the value of the disorder δ ,

As we have shown in Sec.III F the breaking-up length is large for weak disorder and it is of the order of $L^b = 40$ for $\delta \approx 0.4$. Therefore we have restricted ourselves to the disorder range: $0.4 < \delta \leq 1$, which contains all interesting parts of the phase diagram.

A. Phase diagram

The numerically calculated phase diagram as a function of disorder and temperature is already presented in Sec.II in Fig. 2, here we give a detailed analysis of the results. The phase boundary between the ordered and disordered phases is calculated by considering two quantities. Finite-size or percolation transition temperatures, $T_c(L)$, are identified in each sample at the point where the largest connected cluster of the optimal set starts to percolate the finite sample. The distribution of $T_c(L)$ is shown in Fig.3 in the first-order transition regime ($\delta = 0.5$) and in Fig.4 in the second-order transition regime ($\delta = 0.875$).

While for $\delta = 0.875$ the distribution of the transition temperatures is well described by a Gaussian even for relatively small systems, for $\delta = 0.5$ the distributions show deviations from a Gaussian. As we can see in Fig.3 in the first-order regime the distribution for finite L consists of well separated peaks and it becomes (quasi-)continuous only in the thermodynamic limit. Also the

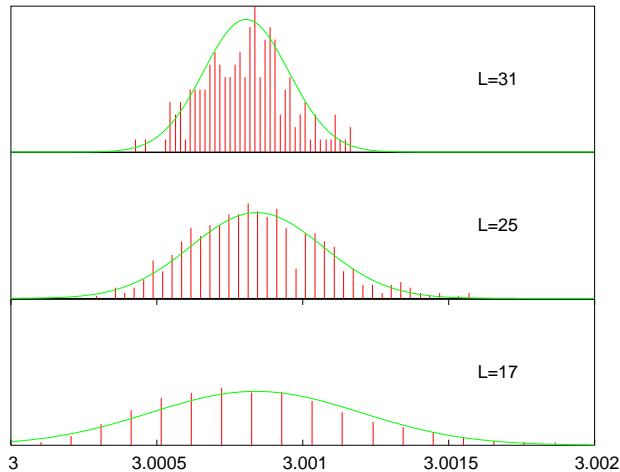


FIG. 3: Distribution of the finite-size percolation transition temperatures in the first-order transition regime at $\delta = .5$ for three different sizes. The Gaussian distributions having the same average and variance are normalized and serve as a guide to the eye..

distributions are non-symmetric and the skewness seems to vanish slowly with the size of the system. It is also evident from Figs.3 and 4 that the finite-size shift of the average transition temperature has a different sign in the two regimes and it is much smaller for a first-order transition in particular if we compare with the variation of the width of the distributions. On the contrary in the second-order transition regime these two characteristics of the distribution are in the same order, see in Fig.4. These observations are in accordance with the scaling picture in Sec. III E, which predicts two different exponents, $\tilde{\nu}$ and ν in the first-order transition regime, whereas in the second-order regime these exponents are the same. However, due to the comparatively small sizes we have and the deviations of the distributions from the Gaussian we could not numerically estimate these exponents.

We have also calculated the transition temperature from the position of the maximum of the averaged specific heat, $C_v(T, L)$, which is expected to be shifted in finite systems as the maxima of $T_c(L)$, as given in Eq.(11). Indeed the numerical results on the specific heat in Fig. 9 at $\delta = 0.875$ are compatible with the same estimate for T_c , as obtained in Fig.4 through the percolation transition temperatures.

As discussed before magnetic order in the system is related to the properties of the largest connected cluster in the optimal set: it has a finite extent in the disordered phase, whereas a finite fraction of sites belongs to this cluster in the ordered phase. The optimal set in the ordered phase, however, can be of two different kinds as far as the structure of isolated points is considered. For weak disorder, $\delta < \delta_{pr}$, or for low temperature, $T < T_{pr}$, the isolated sites form finite clusters. This is always the case in $2d$. In $3d$, however, and this is a new feature of these systems for strong enough disorder and high enough

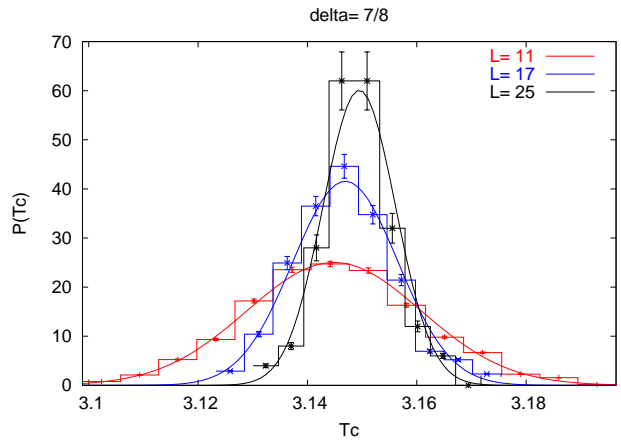


FIG. 4: The same as in Fig.3 in the second-order transition regime at $\delta = 0.875$

temperatures the isolated sites percolate the sample, too. This percolation regime is also indicated in Fig.2 and we argue below that its existence close to T_c is necessary to have a second-order transition in the system. Indeed, the correlation length in the ordered phase is given by the size of the largest connected finite cluster, which is isolated from the giant connected cluster. Since this large finite cluster is embedded into isolated points its size can be divergent at T_c only if the isolated sites percolate the sample. In this way we obtain for the value of the tricritical disorder, δ_t , separating the first- and second-order transition regimes that it satisfies the relation,

$$\delta_t \geq \delta_{pr} . \quad (17)$$

Numerical results which are presented below are in favor of the conjecture that in this relation the equality holds.

For the percolating transition temperature of the isolated sites, $T_{pr}(\delta)$, we make the following calculation. In the dilute model, $\delta = 1$, all the strong bonds, $J_1 = 2J$, are present in the optimal set, provided the temperature is below the value of J_1 . For $T > J_1$, however, in the optimal set there are no dangling bonds, i.e. by increasing the temperature over $T = J_1$ sites which have just one strong bond are removed from the optimal set. Since the dangling bonds are a finite fraction of the bonds³² the non-connected sites become percolating at $T_{pr}(1) = 2J$. For $\delta < 1$ there are also weak J_2 bonds in the system and the removal of one strong dangling bond from the optimal set is accompanied by the removal of some weak bonds at the same time. The average number of removed decorating weak bonds is four which is possible in the temperature range:

$$T_c > T > T_{pr}(\delta) = J_1 + 4J_2 = J(5 - 3\delta) . \quad (18)$$

The numerical results show that at $T_{pr}(\delta)$ in a finite fraction of samples there is a giant cluster of isolated points which spans the finite cube, see in Fig.5.

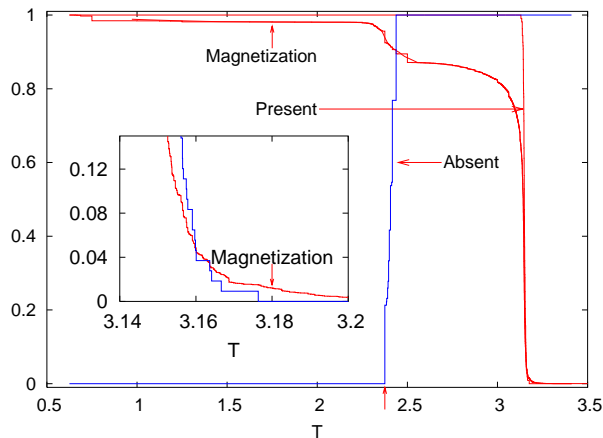


FIG. 5: Magnetization and percolation probabilities of the optimal set (“Present”: for the occupied bonds of the giant cluster; “Absent”: for the isolated sites) of the random model with $\delta = 0.875$, as a function of the temperature in a finite lattice with $L = 24$. The arrow at $T = T_{pr} = 2.375J$ indicates the percolation temperature in Eq.(18) and for $T < T_{pr}$ the magnetization is close to that for ordinary percolation. The singular jumps in the magnetization are a consequence of the discrete form of the probability distribution. Inset: in the vicinity of the transition point the magnetization and the percolation probability of the present bonds are close to each other, the differences are due to finite-size effects.

At the percolation transition temperature there is a sudden change in the structure of the giant connected cluster, which results in singularities in the thermodynamical quantities. As an illustration we show in Fig. 5 the temperature dependence of the magnetization at $\delta = 0.875$, i.e. in the second-order transition regime. The magnetization goes to zero at the phase-transition point, which - in the thermodynamic limit - coincides with the percolation transition of the occupied bonds. For finite systems the magnetization and the probability of having a spanning cluster has small deviations, as illustrated in the inset of Fig. 5. The magnetization has another singular jumps for $T < T_c$, which are due to the discrete form of the disorder. Among these singularities the most pronounced is that around the percolation temperature at $T_{pr} = 19/8$. As seen in Fig. 5 the percolation probability of the isolated sites has a finite value at T_{pr} and it goes to the value of one within a small temperature range. It is expected that by decreasing the disorder to the tricritical value, the singularities at T_c and T_{pr} merge into a new type of tricritical singularity.

B. Order of the transition

To decide about the order of the transition one generally studies the behavior of the latent heat in the system. This type of analysis, however, for the large- q state Potts model is complicated, if the disorder is discrete, as in our

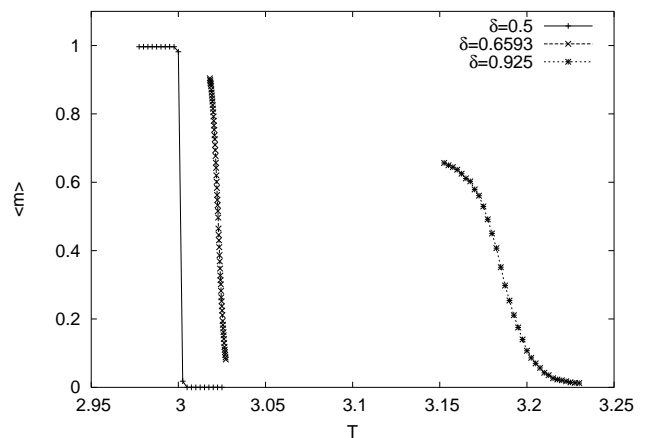


FIG. 6: Temperature dependence of the magnetization in the transition region for $L = 16$ with different strength of disorder. From left to right $\delta = 0.5$ - first-order regime; $\delta_t = 0.6593$ - tricritical point; $\delta = 0.925$ - second-order regime.

case. As already discussed in $2d^{10}$ the internal energy of the system displays discontinuities, both at and outside the critical point. These discontinuities, however, are generally connected to such degeneracies of the optimal set which are related to the removal of finite number of bonds, thus do not modify the global structure of the giant connected cluster. As a consequence these singularities can not be interpreted as a sign of first-order transition. In $3d$ and for the bimodal disorder used in this paper this type of non-generic discontinuities of the internal energy are also present therefore we did not try to make an analysis of this quantity.

Instead we have studied the magnetization in the system, which is defined as the fraction of sites in the largest connected cluster. A jump in the magnetization indicates a fundamental change in the shape of the largest cluster, thus a first-order transition. The magnetization as a function of temperature is shown in Fig.5 for different values of the disorder corresponding to the different transition regimes. A direct measurement of the jump in the magnetization is possible only up to $\delta \leq 0.6$, see in Ref.¹⁹, whereas the lower limit of the second-order transition regime is estimated through the calculation of the fractal dimension of the giant cluster at the transition point, see in Fig.2. This type of analysis at δ_{pr} (see in Sec. IV D) has given a fractal dimension, $d_f^t < 3$, which together with Eq.(17) indicates that the first-order transition regime stops at δ_{pr} .

C. Second-order transition regime

In the second-order transition regime we have made detailed calculations at the disorder $\delta = 0.75, 0.8, 0.875, 0.925$ and at $\delta = 1$. The most detailed studies are performed at $\delta = 0.875$, in which case the largest system is $L = 40$ for the other cases we went

up to $L = 32$. With these investigations our aim was to check universality of the critical properties of the system.

The magnetization exponent, β , and the magnetization scaling exponent, $x = \beta/\nu$, is related to the fractal dimension of the giant cluster, d_f , as $d - x = d_f$. Among these critical parameters it is the fractal dimension which can be determined with the highest precision. To obtain the fractal dimension we considered a reference point of the percolating cluster and measured the mass (number of points) in a shell around the reference point with unit width and radius, r . The average mass, $s(r, L, T)$, is expected to scale close to the transition point: $t = (T - T_c)/T_c \ll 1$ as:

$$s(r, L, t) = L^{d_f-1} \tilde{s}(r/L, tL^{1/\nu}). \quad (19)$$

Generally, one sets the second argument of the scaling function, $\tilde{s}(\rho, \tau)$, to be zero by performing the calculation at the transition temperature, $T = T_c$. In our case T_c is not known exactly, therefore we have used another strategy. For each size we set, $T = \overline{T_c}(L)$, which is the average finite-size (percolation) temperature at the given size. With this choice the second argument of the scaling function, τ is asymptotically constant and thus the scaling function depends only on one parameter: $\tilde{s} = \tilde{s}(r/L)$. Our scaling picture is checked in Fig. 7, in which the scaling plot of the mass in the shell is shown for $\delta = 0.875$. The accuracy of the scaling collapse is measured by the area of the collapse region which is shown in the inset of Fig. 7. It is seen that the optimal scaling collapse is obtained with a fractal dimension, $d_f = 2.40(2)$. This type of analysis of the fractal dimension is repeated for another values of the disorder, too. Since in these cases the available sizes of the systems are comparatively smaller we have somewhat larger errors. The fractal dimensions are shown in the inset of Fig. 2.

The correlation length critical exponent, ν , can be calculated from the shift of the finite-size critical temperature, as given in Eq.(13). However this method has quite a large error. A more accurate estimate can be obtained from the scaling behavior of the magnetization: $m(t, L) = L^{x_m} \tilde{m}(tL^{1/\nu})$. Here we set $x_m = d - d_f$ from the previous calculation and from an optimal scaling collapse as shown in Fig. 8 we have obtained $\nu = .73(2)$. (The area of the collapse region as a function of ν is shown in the inset of Fig. 8.) Note that ν satisfies the rigorous bound for disordered systems³³: $\nu \geq 2/d$.

Finally, we have investigated the behavior of the specific heat at the transition point. As seen in Fig. 9 the maximum of the specific heat is increasing with the size, therefore from the finite-size scaling result: $C_v^{sing}(L) \sim L^{\alpha/\nu}$ one would conclude $\alpha > 0$. This is, however, in conflict with hyperscaling and with the bound of ν in disordered systems. Therefore we tried to fit the numerical data by including a constant in the r.h.s. of the finite-size scaling form. The fit in this way, however, is not satisfactory. In order to get a non-positive α , one should have a constant, which is more than one order of magnitude larger, than the finite-size data. Therefore we

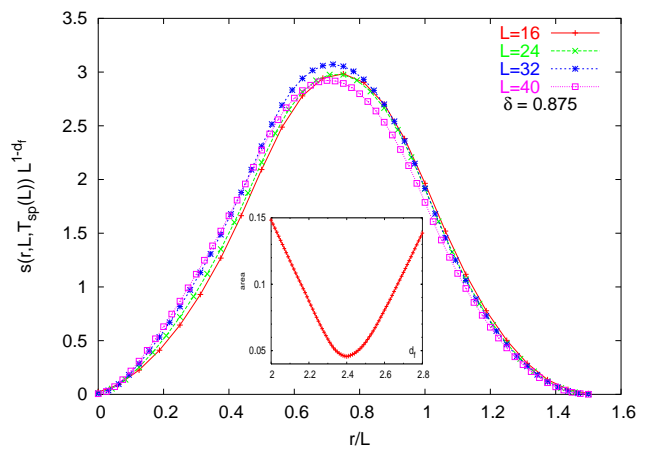


FIG. 7: Scaling plot of the mass of a shell of the infinite cluster, for each size at the average spanning temperature, see text, at $\delta = 0.875$. Optimal collapse is obtained with a fractal dimension, $d_f = 2.40$. Inset: area of the collapse region as a function of d_f .

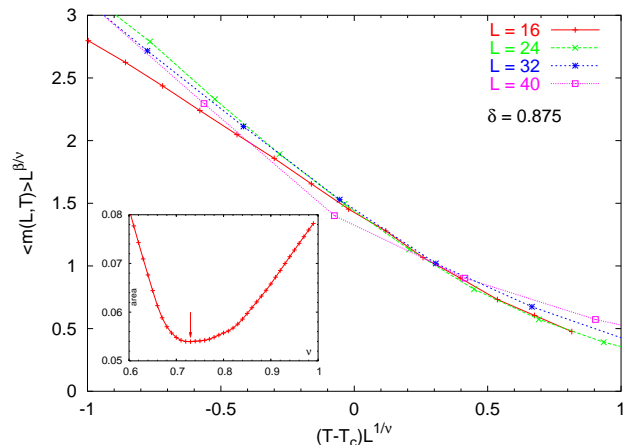


FIG. 8: Scaling plot of the magnetization at $\delta = 0.875$ as a function of the distance from the critical temperature. By fixing $\beta/\nu = d - d_f = 2.4$ the best collapse is obtained with $\nu = .73(2)$. In the inset the area of the collapse region is shown as a function of ν , the arrow indicates the position of the minima.

have concluded that the asymptotic regime of the specific heat is very far from the possibilities of present day numerical calculations.

D. Tricritical transition

Analyzing the structure of the optimal set in the ordered phase we have got a relation between the tricritical disorder and the percolating disorder, as written in Eq.(17). Later we have conjectured that in this relation probably the equality holds, i.e. at the tricritical point

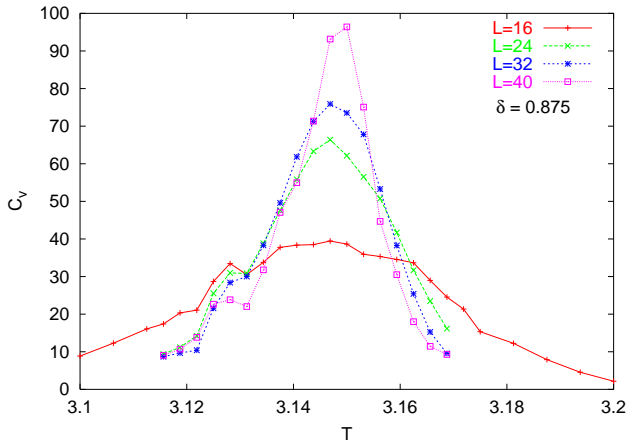


FIG. 9: Finite-size specific heat as a function of temperature at $\delta = 0.875$. According to hyperscaling the maxima of the curves should approach a finite limiting value. The relatively large errors are due to numerical derivation of a piece-wise linear function

three regions (disordered phase, ordered phase and percolating regime) meet. Here we check this conjecture numerically in the following way. We sit on the analytical continuation of the percolation transition line in Eq.(18) for $\delta < \delta_{pr}$ (thus for $T > T_{pr}$) and calculate the finite-size transition point, which is located at such $\delta_t(L)$ for which in half of the samples the giant connected cluster percolates the finite cube. Then we have analyzed the fractal properties of the giant connected cluster and repeated the procedure as described in Sec.IV C for the second-order transition regime. Using the relation about the number of sites in a shell in Eq.(19) and fixing the temperature for each size through $\delta_t(L)$ we have made a scaling analysis as in Fig.7 for the second-order transition regime. According to the results in Fig.10 the giant cluster is a fractal and the best collapse of data is obtained (see inset) with $d_f^t = 2.90(2)$. This value is definitely different from that at a first-order transition, $d_f = d = 3$, and also differs from that in the second-order transition regime. Thus our numerical results are in accordance with the conjecture, that the tricritical disorder is given by

$$\delta_t = \delta_{pr}$$

Our numerical data are very sensitive to the value of δ , and by extrapolating the finite-size results obtained from the best collapse we find $\delta = 0.65930(5)$ and $T = 3.0221(1)$. Furthermore, we obtain the estimate for the anomalous dimension of the tricritical magnetization, $x_m^t = 0.10(2)$.

In order to calculate the correlation length exponent, ν , at the tricritical point we consider the magnetization, $m(t, \tau, L)$, as a function of reduced temperature, t , difference of the tricritical disorder, $\tau = (\delta_t - \delta)/\delta_t$, and the size, L . According to finite-size scaling we

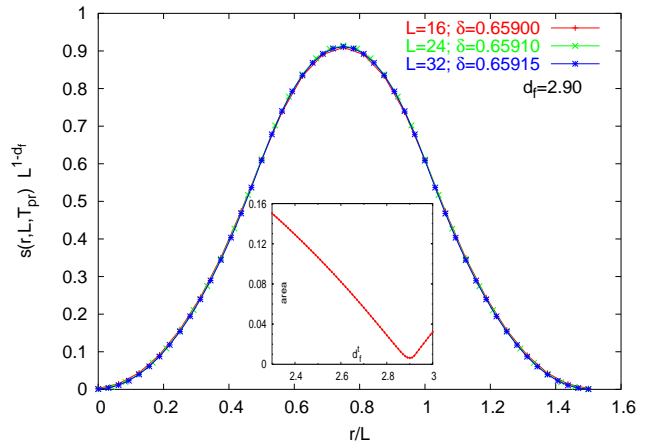


FIG. 10: Scaling plot of the mass of a shell of the infinite cluster analyzed along the percolation transition temperature, Eq.(18). For each size we fix the disorder and thus the temperature as the average spanning temperature, see text. Optimal collapse is obtained with a fractal dimension, $d_f^t = 2.94$. Inset: area of the collapse region as a function of d_f^t .

have $m(t, \tau, L) = L^{-x_m^t} \tilde{m}(\tau L^{1/\nu_\tau}, t L^{1/\nu})$ and by having a disorder $\delta_t(L)$, (thus $\tau(L)$) for each finite size we fix asymptotically the first argument of the scaling function. Consequently from the optimal scaling collapse of $m(t, \tau(L), L) L^{x_m^t}$ we can obtain the correlation length exponent. We noticed that at the tricritical point the estimate for ν is more sensitive to the range in which the collapse is performed. Using the symmetric region indicated in Fig. 11 the minimum of the scaling area in the inset of Fig. 11 is at $\nu = 0.64$. However using an asymmetric window, $-0.1 < (T - T_c) L^{1/\nu} < 0.3$, we obtain a value which is slightly larger than the borderline value $\nu = 2/3$ according to the criterion by Chayes et al³³. Therefore we conclude the estimate of the correlation length exponent at the tricritical point as: $\nu = 0.67(4)$.

The tricritical fixed point of the random bond Potts model in the large- q limit is related to the critical fixed point of the random-field Ising model according to a mapping due to Cardy and Jacobsen⁶. As described in Ref.[6] the interface Hamiltonian of the two problems in the solid-on-solid approximation are equivalent to each other in $d = 2 + \epsilon$ dimension, and this mapping is expected to hold for larger values of d , in particular for $d = 3$. According to the mapping magnetization-like excitations of the RFIM correspond to energy-like excitations in the random bond Potts model. In particular the correlation-length exponent at the tricritical point of the RBPM is conjectured to relate on the critical exponents of the RFIM as

$$\nu = \nu^{RF} / (\beta^{RF} + \gamma^{RF}). \quad (20)$$

For the 3d RFIM with Gaussian disorder recent estimates

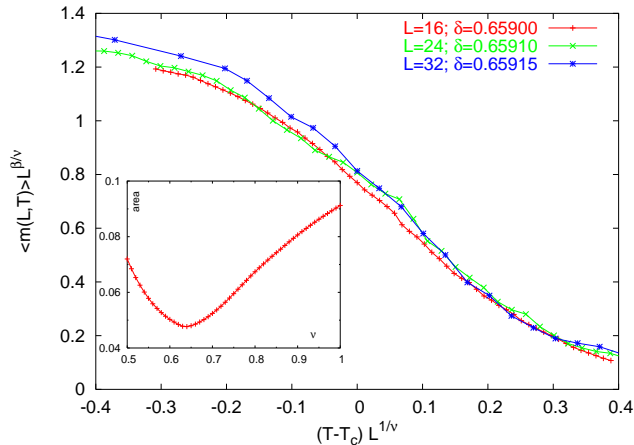


FIG. 11: Scaling plot of the magnetization at the finite-size tricritical disorder as a function of the distance from the tricritical temperature, see text. By fixing $\beta^t/\nu = d - d_f^t = 2.90$ the minimum of the collapse region (see inset) is obtained with $\nu = .64$.

on the critical exponents are³⁴:

$$\nu^{RF} = 1.37(9), \quad \beta^{RF} = 0.017(5), \quad \gamma^{RF} = 2.04(14), \quad (21)$$

which imply through Eq.(20) $\nu = 0.67(2)$, which coincides with our direct calculation. In this way our study of the tricritical singularities lends support to the mapping by Cardy and Jacobsen. The tricritical magnetization exponent, x_m^t , we calculated above can not be predicted by the mapping therefore it gives a completely new piece of information.

Finally, we note that in the spirit of the RG description the number of Potts-states, more precisely $\ln q$, is a dangerous irrelevant scaling variable. Therefore the calculated tricritical exponents are expected to be q -independent and probably universal for any three-dimensional systems in which the first-order transition in the pure systems is softened by tricritical disorder. As a matter of fact, it is much easier to compute the free energy of the Potts model at q infinite, using submodular functions theory, than at q very large. This will make difficult to check the assumption above, at least numerically and in the framework of the Potts model.

V. DISCUSSION

Here we discuss some aspects and possible extensions of our results obtained in the previous Sections.

A. Dynamical behavior for weak disorder

In a random ferromagnetic system having a second-order transition point different dynamical quantities (susceptibility, autocorrelation function, etc.) are singular

outside the critical point and this regime is called the disordered and ordered Griffiths phases³⁵. The singular behavior is due to rare regions which, due to strong disorder fluctuations, are locally in the non-stable thermodynamic phase of the system. It is easy to see that similar effects can be observed outside and at a first-order transition point, as we show in the following for our model with weak disorder. Note, however, that our numerical results concern q infinite, for which no dynamics is defined. Indeed, only the spin-state compatible with the diagram(s) maximizing the function in Eq.(4) are possible, all these states being equiprobable. The analysis below refers to q very large, but finite.

In the disordered Griffiths phase of the random bond Potts model such a rare region is a domain (cube) of linear size l , having only strong couplings, as described in Sec.III B. These regions are indeed rare since they appear with a probability: $P(l) \sim 2^3(l^3 - l^2)$. In such a cluster in equilibrium all the spins are typically in the same state, provided the conditions in Sec.III B are fulfilled. However during a relaxation process they flip into another parallel configuration. Having heat-bath dynamics the relaxation time, t_r , can be estimated in such a way, that in a thermally activated process the cluster should overcome an energy barrier, $\Delta E(l)$, which is the energy of creation an interface in the system. The relaxation time is then given by: $t_r \sim \exp(\beta \Delta E(l))$. Generally the interfacial energy is proportional to the number of sites involved in the interface: $\Delta(l) \sim l^{d-1} \xi_{\perp}$, where ξ_{\perp} is the width of the interface. It is known³⁶ that outside the first-order transition point ξ_{\perp} is finite, whereas at the transition point it is divergent as $\xi_{\perp} \sim l^{\zeta}$ with a thermal wandering exponent: $\zeta = (3 - d)/2$. In particular at $d = 3$ we have a logarithmic divergence. Now calculating the distribution of relaxation times we obtain $P(t_r) \sim \exp[-cst (\ln t_r)^{d/\omega}]$, where $\omega = d - 1$, outside the transition point of the cluster and $\omega = d - 1 + \zeta$, close to the transition point. Then the average autocorrelation function is given by:

$$G(t) \sim \int dt_r P(t_r) \exp(-t/t_r) \sim \exp \left[-cst (\ln t)^{d/\omega} \right], \quad (22)$$

which has a different form at the first-order transition point and in the disordered phase.

B. Effect of the form of disorder

In this paper in the numerical studies we considered bimodal i.e. discrete form of disorder. This was mainly due to technical simplifications. The basic behavior of the system in particular its critical properties are not expected to change using a continuous form of disorder. For example the phase-diagram has the same topology as shown in Fig.2, i.e. disordered and ordered phases and first- and second-order transition regions. The percolation region of the ordered phase also exists and very

probably the tricritical point is located at the meeting point of these three phases or regions. Also the critical singularities at the second-order transition line are very probably disorder independent, as we have already observed in the two-dimensional problem¹⁰. To the same question for the tricritical transition is more difficult to answer. Having in mind that the $3d$ RFIM might have disorder dependent singularities³⁷ the same can be true for the tricritical singularities, due to the mapping as described in Sec.IV D. Finally the discrete nature of the disorder can result in non-physical discontinuities in the internal energy, which are washed out by continuous disorder.

C. Effect of the number of states - q

In the second-order transition regime the critical exponents are q -dependent, which can be seen from the results of numerical investigations^{13,14} and the same scenario holds in two dimensions, too. The tricritical singularities, however, at least those which are related to the energy density, are very probably q -independent and thus 'hyperuniversal'. It would be very interesting to check this statement for another systems, since the Potts model in three dimensions for q finite but very large, seems out of the reach of the usual methods. Finally we mention that the non-physical discontinuities in the internal energy are also absent for finite value of q .

D. Model with correlated disorder

Finally, we consider our model with correlated disorder, in which translational invariance is present in the vertical direction, in which the couplings are constant, J_{\perp} , whereas in the horizontal $2d$ planes the couplings are random, J_{ij} , and strictly correlated in each planes.

This type of columnar disorder is introduced by McCoy and Wu in the $2d$ Ising model³⁸. Due to translational symmetry in the vertical direction the model is conveniently studied in the transfer matrix formalism. Using the extreme anisotropic limit of the model³⁹, when, $J_{\perp}/J_{ij} \rightarrow 0$ the transfer matrix is written into the form: $\mathcal{T} = \exp(-\tau\mathcal{H})$, where τ is the infinitesimal lattice spacing and \mathcal{H} is the Hamiltonian operator of the $2d$ quantum Potts model with random couplings. This latter model can be studied by a strong disorder renormalization group method⁴⁰ which leads to q -independent critical properties. According to numerical results^{40,41} the correlation length critical exponent is $\nu = 1.15(10)$ and the anomalous dimension of the magnetization is $x_m^{an} = 0.97(3)$. This latter result implies that the fractal dimension of the giant anisotropic cluster is given by: $d_f^c = d - x_m^c = 2.03(3)$, and evidently $d_f^c < d_f$. Starting with the anisotropic model we can go to the isotropic model by letting the couplings to be random in the vertical direction, too. Our results indicates that during this process the mass of the largest cluster is increasing, i.e. the creation of new connected parts is more effective than the creation of isolated sites. This result is in accordance with the form of the phase-diagram in Fig. 2, in which due to a similar process the ordered phase has a larger extent with increasing disorder. We note that in $2d$ our numerical results show¹⁰ that $d_f^{an} = d_f$, which let us to conjecture the exact values of the critical exponents in the random bond Potts model. Here we have argued that in $2d$ due to duality the creation and destruction processes play equivalent rôle and therefore the fractal dimension stays unchanged.

This work has been supported by the French-Hungarian cooperation programme Balaton (Ministère des Affaires Etrangères - OM), the Hungarian National Research Fund under grant No OTKA TO34183, TO37323, TO48721, MO45596 and M36803. F.I. thanks for useful discussions with C. Monthus and H. Rieger.

¹ A. B. Harris, J. Phys. C **7**, 1671 (1974).

² Y. Imry and M. Wortis, Phys. Rev. B **19**, 3580 (1979); K. Hui and A.N. Berker, Phys. Rev. Lett. **62**, 2507 (1989).

³ M. Aizenman and J. Wehr, Phys. Rev. Lett. **62**, 2503 (1989); errata **64**, 1311 (1990).

⁴ For a review, see: J.L. Cardy, Physica A **263**, 215 (1999).

⁵ M. Picco, Phys. Rev. Lett. **79**, 2998 (1997); C. Chatelain and B. Berche, Phys. Rev. Lett. **80**, 1670 (1998); Phys. Rev. E **58** R6899 (1998); **60**, 3853 (1999); T. Olson and A.P. Young, Phys. Rev. B **60**, 3428 (1999).

⁶ J.L. Cardy and J.L. Jacobsen, Phys. Rev. Lett. **79**, 4063 (1997), J.L. Jacobsen and J.L. Cardy, Nucl. Phys. B **515**, 701 (1998).

⁷ T. Olson and A.P. Young, Phys. Rev. B **60**, 3428 (1999).

⁸ J.L. Jacobsen and M. Picco, Phys. Rev. E **61**, R13 (2000); M. Picco (unpublished).

⁹ J.-Ch. Anglès d'Auriac and F. Iglói, Phys. Rev. Lett. **90**, 190601 (2003).

¹⁰ M.-T. Mercaldo, J.-Ch. Anglès d'Auriac, and F. Iglói, Phys. Rev. E **69**, 056112 (2004).

¹¹ G. S. Iannacchione, G. P. Crawford, S. Zumer, J. W. Doane, and D. Finotello, Phys. Rev. Lett. **71**, 2595 (1993).

¹² K. Uzelac, A. Hasmy, and R. Jullien, Phys. Rev. Lett. **74**, 422 (1995).

¹³ H.G. Ballesteros, L.A. Fernández, V. Martín-Mayor, A. Muñoz Sudupe, G. Parisi, and J.J. Ruiz-Lorenzo, Phys. Rev. B **61**, 3215 (2000).

¹⁴ C. Chatelain, B. Berche, W. Janke, and P.-E. Berche, Phys. Rev. E **64**, 036120 (2001); W. Janke, P.-E. Berche, C. Chatelain, and B. Berche, Nuclear Physics B **719** 275 (2005).

¹⁵ F.Y. Wu, Rev. Mod. Phys. **54**, 235 (1982).

¹⁶ P.W. Kasteleyn and C.M. Fortuin, J. Phys. Soc. Jpn. **46** (suppl.), 11 (1969).

¹⁷ R. Juhász, H. Rieger, and F. Iglói, Phys. Rev. E **64**, 056122 (2001).

- ¹⁸ J.-Ch. Anglès d'Auriac *et al.*, J. Phys. **A35**, 6973 (2002); J.-Ch. Anglès d'Auriac, in *New Optimization Algorithms in Physics*, ed. A. K. Hartmann and H. Rieger (Wiley-VCH, Berlin 2004).
- ¹⁹ M.-T. Mercaldo, J.-Ch. Anglès d'Auriac, and F. Iglói, Europhys. Lett. **70**, 733 (2005).
- ²⁰ M. Grötschel, L. Lovász, A. Schrijver, *Combinatorica* **1** 169-197 (1981).
- ²¹ For more pictures on the optimal sets at different temperatures see at: <http://www.sa.infn.it/mariateresa.mercaldo/3dcluster.html>.
- ²² Y. Imry and S. K. Ma, Phys. Rev. Lett. **35**, 1399 (1975).
- ²³ S. Wiseman and E. Domany, Phys Rev E **52**, 3469 (1995).
- ²⁴ A. Aharony, A.B. Harris, Phys Rev Lett **77**, 3700 (1996).
- ²⁵ F. Pázmándi, R.T. Scalettar and G.T. Zimányi, Phys. Rev. Lett. **79**, 5130 (1997).
- ²⁶ S. Wiseman and E. Domany, Phys. Rev. Lett. **81**, 22 (1998); Phys Rev E **58**, 2938 (1998).
- ²⁷ A. Aharony, A.B. Harris and S. Wiseman, Phys. Rev. Lett. **81**, 252 (1998).
- ²⁸ D.S. Fisher, Phys. Rev. B **51**, 6411 (1995).
- ²⁹ C. Monthus, and T. Garel, preprint cond-mat/0509479.
- ³⁰ B. Nienhuis and N. Nauenberg, Phys. Rev. Lett. **35**, 477 (1975).
- ³¹ M. E. Fisher and A. N. Berker, Phys. Rev. B **26**, 2507 (1982).
- ³² See c.f. in D. Stauffer and A. Aharony, *Introduction to Percolation Theory*, (Taylor and Francis, London) (1992).
- ³³ J. T. Chayes *et al.*, Phys. Rev. Lett. **57**, 299 (1986).
- ³⁴ A.A. Middleton and D.S. Fisher, Phys. Rev. B **65**, 134411 (2002).
- ³⁵ R. B. Griffiths, Phys. Rev. Lett. **23**, 17 (1969).
- ³⁶ M.E. Fisher, J. Chem. Soc. Faraday Trans. **82**, 1569 (1986).
- ³⁷ N. Sourlas, Comp. Phys. Comm. **121**, 183 (1999).
- ³⁸ B.M. McCoy and T.T. Wu, Phys. Rev. **176**, 631 (1968); **188**, 982(1969); B.M. McCoy, Phys. Rev. **188**, 1014 (1969).
- ³⁹ J. Kogut, Rev. Mod. Phys. **51**, 659 (1979).
- ⁴⁰ F. Iglói, and C. Monthus, Phys. Rep. **412**, 277 (2005).
- ⁴¹ O. Motrunich *et al.*, Phys. Rev. B **61**, 1160 (2000).